International Journal of Recent Engineering Research and Development (IJRERD)
ISSN: 2455-8761
www.ijrerd.com || Volume 11 – Issue 02 || Mar - Apr 2026 || PP. 07-18

In-plane Shear Performance Enhancement of Adobe Masonry via Glass Fiber Mesh Reinforced Earthen Composite: Experimental and Numerical

Xiaojie Gao[1], Yuan Cheng[2], Feng Wu[3]
[1]*Dalian Jiaotong University, School of Transportation Engineering, 794, Huanghe Road, Shahekou District, Dalian 116028, China*
[2]*Dalian Jiaotong University, School of Transportation Engineering, 794, Huanghe Road, Shahekou District, Dalian 116028, China*
[3]*Dalian Jiaotong University, School of Transportation Engineering, 794, Huanghe Road, Shahekou District, Dalian 116028, China*

Abstract: Adobe masonry exhibits inherent shear weakness and high seismic vulnerability. To mitigate these issues, two surface-strengthening techniques are proposed: a Fiber-Reinforced Earthen Matrix (FREM) with modified earthen bonding, and an Epoxy-Fiber-Reinforced Earthen Matrix (EP-FREM) utilizing epoxy resin. Direct shear tests on triplet specimens revealed that FREM and EP-FREM increased shear capacity by approximately 100% and 400%, respectively. Failure mechanism analysis shows that unreinforced and FREM specimens failed via traditional joint shearing, with the latter experiencing rendering delamination. Conversely, EP-FREM restructured the stress transfer path through superior epoxy bonding, shifting the failure mode to compressive splitting and significantly enhancing initial stiffness and ductility. Refined finite element (FE) modeling further quantifies fiber utilization efficiency under parametric variations. Results indicate that reinforcement effectiveness is governed by the reinforcement ratio and interfacial boundary conditions. Specifically, increased fiber spacing induces localized stress concentrations that weaken global confinement, while additional fiber layers improve stress redistribution—though their macroscopic efficiency remains strictly limited by interfacial bond quality. This research elucidates the mechanical synergy of earthen composite systems, providing a robust theoretical basis for their structural application.

Keywords: Adobe masonry, Glass fiber mesh, In-plane shear performance, Surface strengthening, Numerical investigation

1. Introduction

Adobe is one of the oldest building materials, with the advantages of convenient material acquisition and wide distribution. Nevertheless, adobe structures suffer from low tensile and shear strength as well as weak earthquake resistance. Common retrofitting approaches for adobe structures typically use cement mortar, steel mesh, or timber battens [1]–[3]. Yet field applications and studies indicate that conventional methods suffer from poor physical and mechanical compatibility. For example, cement mortar and natural earthen matrix differ greatly in elastic modulus and shrinkage rate, and interface debonding is very likely to occur under inconsistent deformation **Error! Reference source not found.**. In addition, the high water absorption of natural earthen materials will lead to insufficient hydration and curing of surface mortar, thereby causing strength attenuation. Such interface compatibility defects seriously limit the long-term effectiveness of traditional strengthening technologies for adobe buildings, and it is urgent to explore new strengthening technologies with better compatibility.

In recent years, fiber composite materials have shown great potential in the strengthening of masonry due to their excellent characteristics such as light weight, high strength and strong corrosion resistance [6]–[8].Numerous studies have found that the shear and seismic performance of masonry walls strengthened with fiber composite materials such as FRP and FRCM have been effectively improved [9]–[14]. Research also indicates that the strengthening effect of FRP is significantly affected by the performance of the base material, and there are obvious fluctuations in the strengthening effect when applied to adobe masonry [15], [16].

Although fiber composite materials have achieved certain results in masonry strengthening, research on the strengthening of adobe masonry is still relatively insufficient. Compared with conventional sintered brick and concrete block masonry, adobe masonry has weaker mechanical properties such as shear and compressive resistance [17], [18]. Conventional cement mortar is difficult to form an effective stress transfer interface with the natural earthen matrix, resulting in premature debonding of the strengthening layer [19], **Error! Reference source not found.**.Accordingly, it is necessary to further explore the applicability of fiber composite materials

in adobe masonry, especially to develop modified matrix materials with better mechanical compatibility with the natural earthen matrix to maximize the strengthening efficiency for adobe buildings.

Aiming at the above problems of interface compatibility and insufficient shear performance, this study takes unreinforced adobe masonry specimens, FREM strengthened specimens and EP-FREM strengthened specimens as research objects to carry out direct shear tests, and systematically analyzes the improvement effect of two strengthening methods on the shear performance of adobe masonry. The action mechanisms of the two strengthening methods are revealed by comparing the core mechanical characteristics such as load-displacement curves and failure modes of each specimen. Based on the test results, a refined three-dimensional finite element macroscopic model is established to conduct parametric analysis on the stress utilization efficiency of fiber mesh, and quantitatively discuss the influence laws of fiber spacing, laying layers and single/double-sided arrangement on the peak bearing capacity and internal stress distribution of the system. This study aims to provide a reliable test basis and theoretical support for the seismic restoration of adobe buildings and fiber composite strengthening technology.

2. Experimental method

2.1 Material Properties

The adobe masonry and mortar used in this test were prepared from the same test natural earthen. The selection of the test natural earthen was based on references [21], with 53.8% coarse particles, 16.12% silt particles, a liquid limit of 39.8%, and a plasticity index of 24.

The alkali-resistant glass fiber mesh used in the test has a grid size of 10 mm×10 mm and an area density of 170 g/m². Tensile tests were conducted on six single bundles of fibers. The results indicate that the average ultimate tensile force is 1393.13 N, the ultimate tensile strength is 303.91 MPa, and the elastic modulus is 8104.29 MPa.

The surface layer matrix adopts waterborne polyurethane (WPU) modified natural earthen material [22]. After preparing the solution according to the volume ratio of water to polyurethane of 1:4, it is mixed with natural earthen at a mass ratio of 1:4. After standard curing for 28 days, the ultimate compressive strength of the modified natural earthen is measured to be 5.6 MPa, the elastic modulus is 182.5 MPa, and the Poisson's ratio is 0.3.

For the EP-FREM system, two-component epoxy resin is used as the interface impregnation and bonding agent. The mixing viscosity of the epoxy resin is 45000 mPa·s, and its tensile strength and elastic modulus after curing are 70 MPa and 3500 MPa, respectively.

2.2 Test Grouping and Specimen Preparation

With reference to the European masonry test standard Methods of test for masonry (EN 1502-3), this study designed and fabricated triplet adobe masonry specimens to evaluate the in-plane shear performance, including unreinforced adobe masonry, FREM strengthened specimens and EP-FREM strengthened specimens. The size of the adobe masonry is 200 mm×90 mm×170 mm, including two horizontal mortar joints with a thickness of 10 mm, as shown in Figure 1. To ensure the statistical validity and repeatability of the test results, 3 parallel specimens are set in each group.

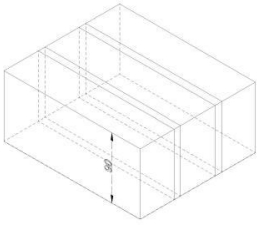

a) Unreinforced specimen

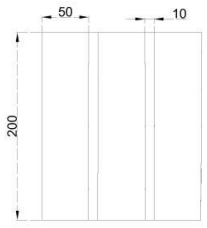

b) Front view of unreinforced specimen

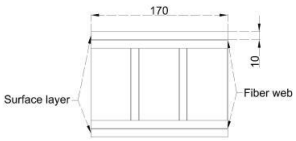

c) Top view of FREM reinforced specimen

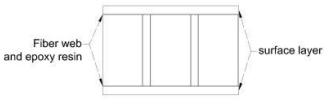

d) Top view of EP-FREM reinforced specimen

Figure 1: Schematic of the Specimen

The strengthening was carried out on the surface after the original adobe specimens were molded and naturally cured for 28 days. In the FREM group, the fiber mesh was pressed into a 10 mm-thick uncured WPU modified natural earthen surface layer, and then covered with a 10 mm-thick surface layer, with a strengthening area of 200 mm×170 mm. In the EP-FREM group, epoxy resin primer was first brushed on the masonry surface, then glass fiber mesh impregnated with epoxy resin was laid, and after preliminary curing for about 12 hours, a 10 mm-thick WPU modified natural earthen surface layer was applied to form a composite anchoring system.

2.3 Test Device and Loading Protocol

A SUNS-300 microcomputer-controlled electro-hydraulic servo universal testing machine was used as the vertical load application and displacement acquisition device for the in-plane shear test of adobe masonry. With reference to the triplet shear test mode of EN 1052-3, the specimen was placed on a custom rigid steel pedestal. As illustrated in Figure 2, symmetrically arranged rectangular steel blocks are used at the bottom to support the adobe bricks on both sides of the masonry. A 12-mm-thick rigid steel plate at the top center uniformly transfers the vertical load, thereby forming a pure shear stress state between the mortar and the blocks.

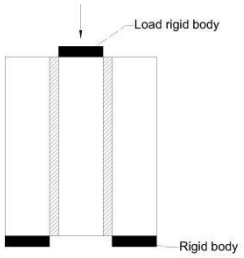

Figure 2: Loading Method of Adobe Masonry

Tests were conducted under displacement-controlled loading. Before formal loading, pre-loading was carried out, and paused when it reached about 5% of the estimated ultimate bearing capacity to eliminate the physical gaps between devices, compact the contact surface, and verify the reliability of the data acquisition system and specimen fixation. After confirmation, monotonic continuous loading was carried out at a constant rate of 1.5 mm/min until the specimen failed. During the test, the load sensor and displacement meter built in the testing machine synchronously and continuously recorded the load and displacement responses. When any obvious vertical through crack appeared on any shear surface or the bearing capacity dropped sharply, the specimen was judged to have shear failure and the test was stopped.

3. Test Results and Analysis

3.1 Failure Modes and Mechanisms

The failure modes of the three groups of specimens under direct shear load are shown in Figure 3. The test results show that the surface strengthening system significantly changes the failure mode of adobe masonry. The unreinforced specimen presents typical brittle shear failure. Its failure is mainly concentrated at the mortar joints, which, as the weakest link in adobe masonry , first cracks and propagates rapidly, eventually leading to specimen failure, indicating that the bonding strength between mortar and adobe bricks is much lower than that of the natural earthen material itself, which is consistent with the common masonry failure characteristics. The FREM specimen shows a progressive failure mode of "surface layer debonding-mortar joint shear". At the initial stage of loading, the surface layer and the masonry bear the load together: with the increase of shear deformation, due to the limited interface bonding capacity between the modified natural earthen surface layer and the natural earthen matrix, the surface layer debonds and falls off, and then vertical cracks appear in the internal mortar joints. The peeled strengthening surface layer remains basically intact, indicating that the high-strength tensile performance of the fiber mesh is limited by the interface bonding failure and cannot be fully exerted. The failure mode of the EP-FREM strengthened specimen has undergone a fundamental change, from mortar joint shear failure to vertical through cracking on the side of the adobe, showing compressive failure characteristics. The high-modulus epoxy resin forms a high-strength bonding layer on the masonry surface, and the external shear load can be effectively transferred to the internal bricks. This demonstrates that the EP-FREM system effectively reshapes the stress transfer path and avoids the premature failure of mortar joints in adobe masonry.

a) Unreinforced b) FREM c) EP-FREM

Figure 3: Shear failure pattern of adobe masonry

3.2 Load-Displacement Response and Shear Bearing Capacity

The displacement-load curves of each group of adobe masonry specimens are shown in Figure 4. (UN represents the unreinforced specimen; FREM represents the FREM specimen: EP-FREM represents the EP-FREM specimen).It can be seen from the curves that the shear bearing capacity of the EP-FREM strengthened specimen is the most significantly improved. The load-displacement curve of unreinforced masonry specimens displays typical linear elastic characteristics at the initial loading stage. After reaching the peak load, the bearing capacity degrades rapidly, exhibiting significant brittle failure characteristics. The FREM strengthened specimen shows similar linear characteristics at the initial stage, and the linear stage is significantly prolonged due to the synergistic effect of fiber mesh and modified natural earthen mortar; the peak load of the specimen reaches 3331 N, which is about 102% higher than that of the unreinforced group, and the peak displacement increases to 3.74 mm. After reaching the peak load, due to the progressive debonding of the surface layer, the curve enters the softening stage and shows a certain plastic deformation capacity. The EP-FREM system has the most significant improvement in shear bearing capacity, with a peak load of 8846 N, an increase of about 437%.Its initial stiffness is close to that of the original masonry at the initial stage of loading, but with the development of cracks, epoxy resin and glass fiber mesh begin to bear the main tensile stress, and the curve shows obvious stiffness strengthening characteristics. The peak displacement reaches 4.52 mm, and the bearing capacity and energy dissipation capacity of adobe buildings are essentially improved.

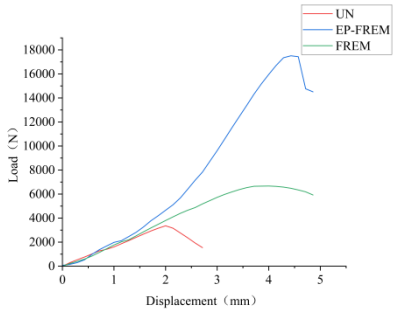

Figure 4: Load-Displacement Curve of Adobe Masonry under Shear

In summary, the significant difference in the macroscopic mechanical properties of the two composite strengthening materials on adobe masonry is essentially derived from the difference in fiber-matrix interface bonding strength and stress transfer efficiency. In the EP-FREM system, epoxy resin effectively inhibits the relative interface slip by virtue of its high bonding with the natural earthen matrix and its own high modulus characteristics. This high-strength interface anchoring mechanism fully stimulates the bridging and crack-resistance potential of the glass fiber mesh, thereby achieving a substantial leap in the shear performance of adobe masonry.

4. Numerical Simulation and Parametric Analysis

4.1 Finite Element Model

A refined three-dimensional finite element model was established to reveal the interface synergistic working mechanism observed in the test. The geometric size of the model is consistent with the test, with adobe bricks of 200 mm×90 mm×50 mm, surface layer of 200 mm×90 mm×170 mm, and the equivalent thickness of glass fiber mesh is 0.1 mm. According to the mesh size partitioning principle presented in the existing literature

[23], the global characteristic element size for bricks, mortar, surface layer and fiber mesh is set to 10 mm, achieving a favorable balance between computational accuracy and efficiency.

The material properties of natural earthen and polyurethane-modified surface layers are parameters obtained from experiments [21]. The elastic modulus, ultimate compressive strength, and ultimate tensile strength are 72.3 MPa and 182.5 MPa, 2.0 MPa and 5.6 MPa, and 0.18 MPa and 0.49 MPa, respectively. The concrete damaged plasticity (CDP) model is adopted for both natural earthen and the surface layer matrix to simulate their compressive crushing and tensile cracking behavior. Figures 5a and 5b present the tensile and compressive stress–strain relationships of the two earthen materials, respectively (NE denotes natural earthen, and WPU denotes polyurethane-modified earthen).

a) Tensile b) Compressive

Figure 5: Tensile and compressive stress-strain models of natural earthen and pu-modified earthen

Damage variables dt and dc ranging from 0 to 1 are used to quantify the degradation of elastic stiffness. A value of 0 corresponds to the undamaged state, while a value of 1 represents complete loss of strength. Dc and dt satisfy the basic equations (1) and (2), in which $\sigma_t$is the tensile stress, $\sigma_c$is the compressive stress, $\varepsilon_t$is the tensile strain, $\varepsilon_c$is the compressive strain, $\varepsilon_t^{pl}$is the equivalent tensile strain, and $\varepsilon_c^{pl}$is the equivalent compressive strain.

$$\sigma_t = (1-dt)\, E_0 (\varepsilon_t - \varepsilon_t^{pl}) \quad (1)$$

$$\sigma_c = (1-dc)\, E_0 (\varepsilon_c - \varepsilon_c^{pl}) \quad (2)$$

For the critical interfacial interaction, tie constraints are adopted between the fiber mesh, surface layer, and masonry matrix in the EP-FREM model to simulate the excellent interfacial impregnation and bonding performance of epoxy resin. In contrast, the FREM model uses a cohesive contact model based on the traction-separation law to characterize the bond-slip behavior, whose tangential bond-slip constitutive relationship is shown in Figure 60. Vertical displacement loads are applied through a top rigid plate, with a displacement of 4 mm for the unstrengthened group and 6 mm for the strengthened group.

a) Natural earthen and natural earthen b) Natural earthen and polyurethane-modified earthen

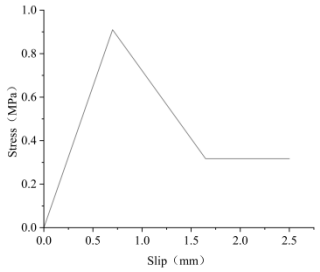

c) Polyurethane-modified earthen and fiber mesh

Figure 6: Bond-slip curve

4.2 Model Validation and Error Analysis

Figure 7 compares the test values and numerical simulation results of the load-displacement curves of each group of specimens. The comparative analysis shows that the finite element model successfully reproduces the larger initial shear stiffness of the strengthened specimens compared with the unreinforced specimens in the elastic stage, verifying the effective synergistic working mechanism of the modified natural earthen surface layer and glass fiber mesh at the initial stage of loading. At the same time, the model also shows the ductility improvement characteristics caused by the constraint effect of fiber mesh on the propagation of internal microcracks after reaching the peak.

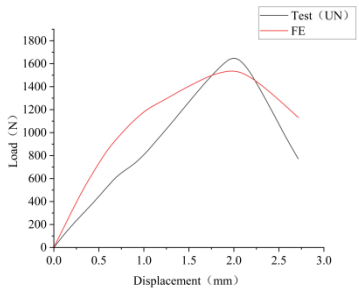

a) Unreinforced

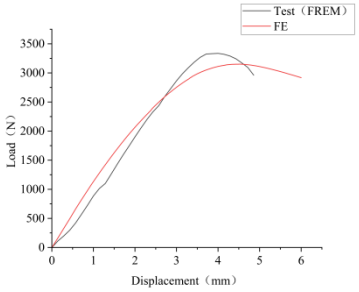

b) FREM

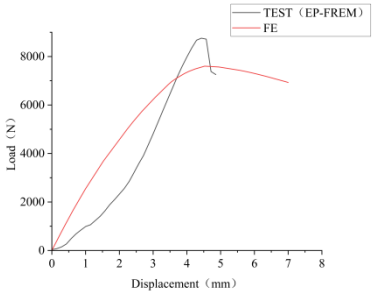

c) EP-FREM

Figure 7: Numerical validation of load-displacement curve

Based on the verified model, the Von Mises stress contours of the specimens at the peak state are extracted for micromechanical analysis, as shown in Figures 8 to 10. The unreinforced adobe masonry specimen shows low stress characteristics as a whole, the stress is mainly concentrated on the upper part of the middle brick and the lower part of the bricks on both sides, and the mortar joint is in the main stress state of pure shear, with a significantly low stress level. Since the mortar joint bonding strength is much lower than the brick strength, the shear stress it bears has approached its own bonding bearing limit, eventually leading to the inability to fully transfer and diffuse the stress to the external bricks, and the compressive and shear properties of the bricks themselves cannot be effectively exerted. The shear stress of the FREM strengthened specimen can be directly transferred to the whole specimen through the strengthening layer. Limited by the limited bonding capacity between the polyurethane surface layer and the masonry matrix, there is micro-slip between the surface layer and the bricks, and the force transfer efficiency has certain loss, so the brick stress increase is limited. Under the high-strength interface action of epoxy resin, the EP-FREM strengthened specimen achieves efficient

collaboration between the matrix and the strengthening system. The fiber mesh becomes the key to bear the main tensile and shear stress, and its peak stress reaches 300% of the fiber stress of the FREM specimen.

In conclusion, both EP-FREM and FREM strengthening methods can effectively improve the shear bearing capacity of adobe masonry specimens through the mechanism of stress sharing and path optimization.

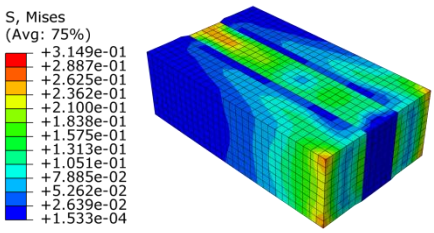

Figure 8: Stress contour of unreinforced specimen

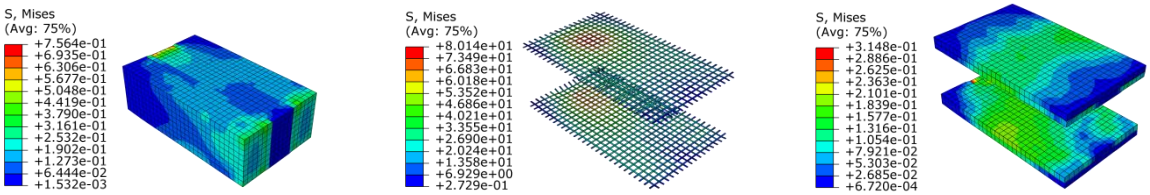

a) Adobe masonry b) Fiber c) Surface layer

Figure 9: Stress contour of FREM reinforced specimen.

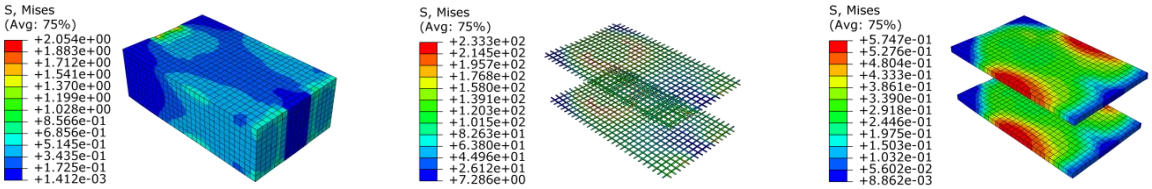

a) Adobe masonry b) Fiber c) Surface layer

Figure 10: Stress contour of EP-FREM reinforced specimen

4.3 Parametric Analysis and Fiber Utilization

To explore the synergistic stress and load sharing mechanism of fiber mesh in the composite strengthening system, fiber spacing (FS20), fiber layers (FL2) and strengthening surfaces (single/double-sided) (SS-S) are selected as core variables for parametric analysis. The test grouping details, peak load, peak displacement and other values are summarized in Table 1. To quantitatively evaluate the stress efficiency of fibers, fiber utilization is defined as the ratio of the maximum tensile stress actually borne by the fiber mesh under load to its ultimate tensile strength.

Table 1: Parametric analysis groups and numerical results

Specimen ID	Number of fiber layers	Fiber spacing (mm)	Number of face sheet layers	Peak load (N)	Peak displacement (mm)	Stiffness (N/mm)
FREM	1	10	2	3149	4.4	715.6
FREM-FS20	1	20	2	3098	3.9	794.3
FREM-FL2	2	10	2	3394	4.7	722.2
FREM-SS-S	1	10	1	2395	4.0	598.7
EP-FREM	1	10	2	7634	4.5	1696.4
EP-FREM-FS20	1	20	2	5831	4.2	1388.3
EP-FREM-FL2	2	10	2	9923	5.2	1908.2
EP-FREM-SS-S	1	10	1	5796	4.0	1449.0

4.3.1 Influence of Fiber Spacing

Expanding the laying spacing of glass fiber mesh from 10 mm to 20 mm will lead to a significant decrease in the effective fiber mesh ratio of the system. The simulation results show that after the natural earthen matrix is damaged and cracked, the external load is forced to concentrate and transfer to the sparser fiber network. This load transfer mechanism leads to a sharp increase in the tensile stress of a single fiber. Compared with the reference group, the maximum fiber stress of FREM-FS20 and EP-FREM-FS20 specimens increases by 60% and 10% respectively, and the fiber utilization reaches 44% and 86% respectively, as illustrated in Figures 11b and 12b.Meanwhile, this passive improvement of local utilization weakens the overall constraint efficiency of the system. As can be seen from Figures 13, 14 and Table 1, the increase in fiber spacing causes the specimen to enter the plastic damage stage prematurely, the peak load of FREM-FS20 decreases slightly by 2%, while the peak load of EP-FREM-FS20 decreases significantly by about 24%. This indicates that excessive fiber spacing will lead to local stress concentration, thereby weakening the inhibition effect of the strengthening layer on the evolution of adobe masonry cracks.

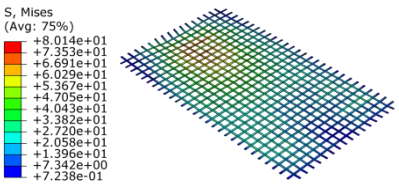

a) FREM

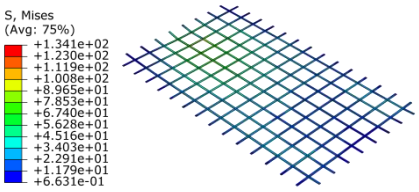

b) FREM-FS20

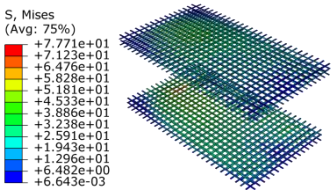

c) FREM-FL2

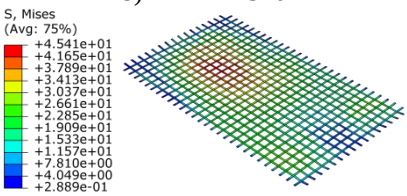

d) FREM-SS-S

Figure 11: Fiber stress contour for parametric analysis

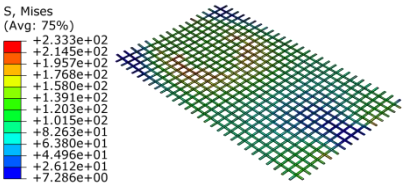

a) EP-FREM

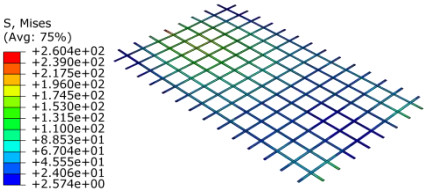

b) EP-FREM-FS20

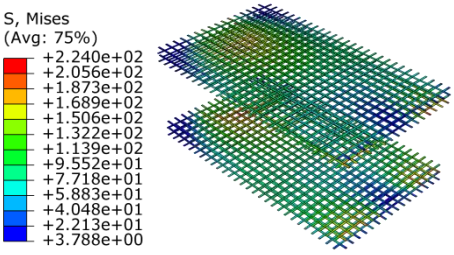

c) EP-FREM-FL2

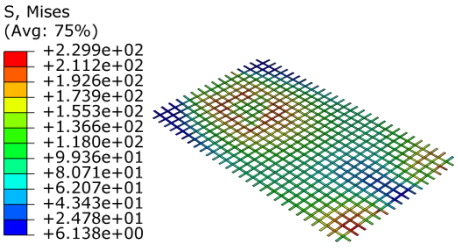

d) EP-FREM-SS-S

Figure 12: Fiber stress contour of EP-FREM in parametric analysis

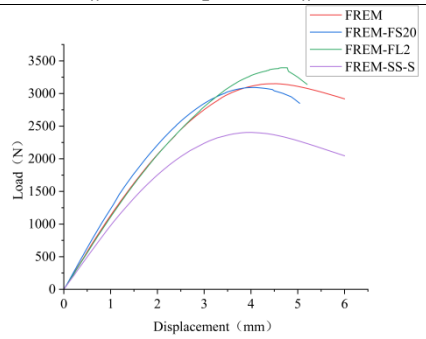

Figure 13: Load-displacement curves of FREM parametric specimens

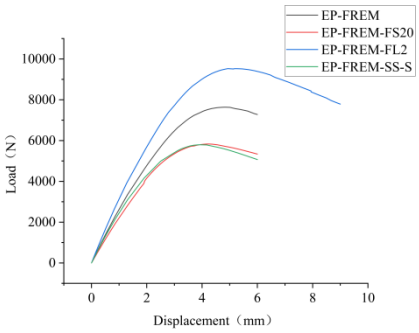

Figure 14: Load-displacement curves for EP-FREM parametric analysis

4.3.2 Influence of Fiber Layers

Adding a layer of fiber composite surface layer to the reference system greatly improves the equivalent fiber mesh ratio of the strengthening system. Figures 11c and 12c show that under the synergistic bearing of double-layer fibers, the external load is distributed more uniformly, so that the single fiber stress of FREM-FL2 and EP-FREM-FL2 specimens is reduced to 96% of the control group, and the utilization rate is reduced to 25% and 74% respectively. In terms of bearing capacity, as shown in Figures 13, 14 and Table 1, the increase in fiber layers shows a significant difference in the growth rate of the two systems. The peak load of the EP-FREM system increases significantly by about 30%, while that of the FREM system only increases by 8%. Combined with the surface stress distribution in Figure 15, it can be seen that even if the number of fiber layers is increased in the FREM system, the overall surface stress level is still low and the distribution lacks gradient change. This phenomenon reveals that interface bonding stiffness is the controlling prerequisite for determining fiber reinforcement efficiency. Due to the bonding defects between the polyurethane modified surface layer and the natural earthen matrix, stress transfer is seriously lost at the interface. In the inefficient bonding state, blindly increasing the amount of fiber cannot achieve a proportional increase in bearing capacity. Instead, the EP-FREM system converts the mechanical properties of double-layer fibers into an improvement in overall stiffness and bearing capacity by virtue of the excellent interface anchoring of epoxy resin.

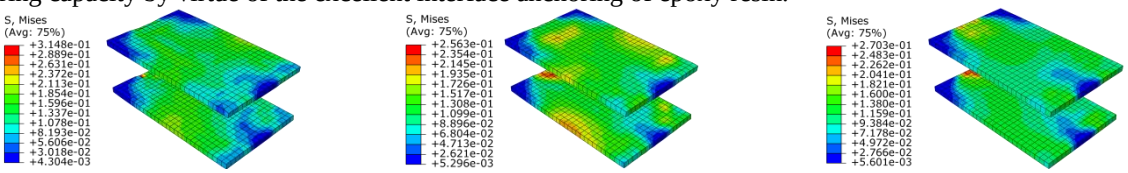

a) FREM b) FREM-FS20 c) FREM-FL2

Figure 15: Surface stress contours of FREM, FREM-FS20 and FREM-FL2

4.3.3 Influence of Single-Sided Strengthening

After replacing the double-sided surface layer with single-sided strengthening, the interface shear transfer efficiency of the composite system is the key factor to ensure the bearing capacity. Under the single-sided stress condition, the maximum tensile stress borne by the single-sided fiber mesh in the two systems not only fails to double as expected, but decreases significantly compared with the double-sided condition. The single-sided fiber stress of FREM and EP-FREM systems decreases by 43% and 33% respectively. This reveals that the single-sided interface needs to bear all the shear load transfer, which is very easy to induce serious interface slip and

local degradation. Once the interface slips, the stress transfer path between the natural earthen matrix and the strengthening layer is partially interrupted, resulting in the premature failure of the matrix under low load, and the tensile potential of the fiber mesh cannot be further stimulated.

The FREM system has a weak bonding stiffness between the modified natural earthen surface layer and the matrix, and the interface force transfer efficiency decays rapidly, resulting in a stress drop of up to 43%， as illustrated in Figure 11d. The EP-FREM system effectively resists interface degradation under high shear load by virtue of the high-strength interface bonding of epoxy resin, so that the single-sided fiber stress drop is controlled at 33%, and the stress diffusion range is relatively wider as illustrated in Figure 12d.This further confirms that under single-sided stress, excellent interface bonding is the core key to delaying interface slip and avoiding interruption of force transfer path.

5. Conclusions

In this paper, the direct shear test combined with refined three-dimensional finite element method is used to compare and study the influence law and interface action mechanism of two glass fiber mesh composite systems, namely waterborne polyurethane modified natural earthen surface layer (FREM) and epoxy resin bonded surface layer (EP-FREM), on the in-plane shear performance of adobe masonry. The main research conclusions are as follows:

(1) Both composite surface strengthening technologies effectively improve the in-plane shear bearing capacity and ductility of adobe masonry. Compared with the unreinforced specimen, the peak shear load of FREM and EP-FREM strengthened specimens is increased by about 102% and 437%, respectively. Under the constraint of fiber mesh, the linear elastic response stage of the specimen is prolonged, and the failure mode changes from brittle shear to ductile failure with certain energy dissipation capacity.

(2) Interface bonding performance directly affects the failure mode of strengthened adobe masonry. Due to the insufficient interface bonding strength of the surface layer, the FREM specimen undergoes interface slip and debonding in the middle and late stages of loading, and the final failure is still controlled by the shear failure of the mortar joint. Relying on the high-strength impregnation bonding of epoxy resin, the EP-FREM system effectively inhibits the relative interface slip, changing the failure mode from mortar joint shear to vertical compressive splitting of the block itself, avoiding the premature failure of the weak link of adobe buildings.

(3) The three-dimensional macroscopic finite element model reveals that the interface force transfer efficiency determines the exertion degree of the high-strength characteristics of fibers. The stress analysis at the peak state shows that the maximum tensile stress borne by the fiber mesh in the EP-FREM system reaches 3 times that of the FREM system. The high-stiffness interface significantly improves the internal stress redistribution of adobe masonry, enabling the shear load to be efficiently transferred to the fiber mesh and maximizing the mechanical potential of the strengthening system.

(4) Parametric analysis shows that the fiber mesh ratio and interface boundary conditions significantly affect the fiber stress distribution. Increasing the fiber spacing to 20 mm will lead to local stress concentration, reducing the bearing capacity of the EP-FREM system by about 24%. Under inefficient bonding conditions (such as FREM specimens), increasing the number of fiber layers has a limited increase in bearing capacity. Under strong anchoring conditions (such as EP-FREM specimens), the bearing capacity can be increased by 30%. This demonstrates that good interface bonding is the controlling prerequisite for the collaborative bearing of multi-layer fibers.

(5) The micro-slip mechanism under asymmetric strengthening boundary has important guiding significance for practical repair engineering of adobe buildings. Under the single-sided stress condition, the force transfer area is halved, leading to a sharp increase in interface shear load, which is very easy to induce premature interface slip and interruption of force transfer path, resulting in a decrease in single-sided fiber stress instead of an increase. Therefore, in practical single-sided strengthening engineering of adobe buildings, interface agents with excellent shear and peeling resistance must be preferred to delay the occurrence of force transfer bottlenecks.

References

[1] Mirabi Banadaki, H., Morshed, R., & Eslami, A. In-plane cyclic performance of adobe walls retrofitted with near-surface-mounted steel rebars. Engineering Structures.2019, 194, 106–119. https://doi.org/10.1016/j.engstruct.2019.05.049

[2] Illampas, R., Silva, R. A., Charmpis, D. C., Lourenço, P. B., & Ioannou, I. Validation of the repair effectiveness of clay-based grout injections by lateral load testing of an adobe model building. Construction and Building Materials.2017, 153,174–184. https://doi.org/10.1016/j.conbuildmat.2017.07.054

[3] Reyes, J. C., Smith-Pardo, J. P., Yamin, L. E., Galvis, F. A., Angel, C. C., Sandoval, J. D., & Gonzalez, C. D. (2019). Seismic experimental assessment of steel and synthetic meshes for retrofitting heritage earthen structures. Engineering Structures, 198. https://doi.org/10.1016/j.engstruct.2019.109477

[4] Zhang, L., Zhou, T., Zhang, Z., Tan, W., & Liang, Z. Near-surface-mounted retrofitting of adobe walls using different materials: Evaluation of seismic performance. Structures. 202354, 1149–1163. https://doi.org/10.1016/j.istruc.2023.05.137

[5] Deng, S., Zhang, Y., He, B., & Xie, L. (2023). Experimental study of the effects of surface roughness and coatings on bonding at the interface between adobe and cement mortar. Materials and Structures/Materiaux et Constructions, 56(5). https://doi.org/10.1617/s11527-023-02191-z

[6] Vegera, P., Grynyova, I., Blikharskyy, Z., Khmil, R., & Korobko, O. (2025). Shear Deformability of Reinforced Concrete Beams Strengthened with the FRCM System. In Springer Proceedings in Materials (Vol. 61, pp. 449–457). Springer. https://doi.org/10.1007/978-3-031-72955-3_45

[7] Alecci, V., Ayala, G., Fernandez, L., De Stefano, M., Galassi, S., & Stipo, G. (2026). Bond Performance of FRCM and FRP Composite Materials on Hollow Concrete Blocks. Lecture Notes in Civil Engineering.2026, 778 LNCE, 1414–1422. https://doi.org/10.1007/978-3-032-09387-5_137

[8] LI, Y., YIN, S., DAI, J., & CHEN, P. (2025). Research on Seismic Performance of Earthquake-damaged Bridge Pier Columns Strengthened with TRC. Zhongguo Gonglu Xuebao/China Journal of Highway and Transport, 38(7), 195–208. https://doi.org/10.19721/j.cnki.1001-7372.2025.07.015

[9] J. Hu, Experimental study on axial compression performance of masonry columns strengthened with ECC and FRP cloth, (Master's thesis, Zhengzhou University)(2023). DOI: 10.27466/d.cnki.gzzdu.2023.003814.

[10] Santa-Maria, H., & Alcaino, P. (2011). Repair of in-plane shear damaged masonry walls with external FRP. Construction and Building Materials, 25(3), 1172–1180. https://doi.org/10.1016/j.conbuildmat.2010.09.030

[11] Micieli, A., Mauro, M., Mazzuca, P., & Ombres, L. (2025). Strengthening of Irregular Stone Masonry Columns with FRCM Systems: Experimental Assessment and Analytical Validation. Lecture Notes in Civil Engineering, 753 LNCE, 53–68. https://doi.org/10.1007/978-3-032-05032-8_5

[12] Sun, X., Shi, P., Zhu, H., Dong, Z., Mu, B., & Soh, C. K. (2025). Shear performance of brick masonry walls strengthened by deep structural repointing using FRP reinforcement. Journal of Building Engineering, 111. https://doi.org/10.1016/j.jobe.2025.113187

[13] Ceroni, F., Lignola, G. P., Prota, A., & Saviano, F. (2025). Experimental investigation on FRCM strengthened tuff masonry walls. Construction and Building Materials, 504. https://doi.org/10.1016/j.conbuildmat.2025.144533

[14] Yin, S., Qu, F., Wang, F., & Wang, B. (2023). Study on seismic performance and analysis of shear bearing capacity of damaged brick masonry walls reinforced by single-sided TRC. Jianzhu Jiegou Xuebao/Journal of Building Structures, 44, 107–115. https://doi.org/10.14006/j.jzjgxb.2023.S2.0011

[15] Wang, X., Shang, H., Lu, Z., Xiao, Z., & Xu, S. (2025). A Review on the Bonding Performance of FRP Bars to Concrete: Mechanisms, Testing Methods, and Influencing Factors. Cailiao Daobao/Materials Reports, 39(17). https://doi.org/10.11896/cldb.24070179

[16] T. MA, Experimental Study on the Bond Performance of the CFRP-ECC-concrete composite interface [D].(Master's thesis, Changan University)(2024).DOI:10.26976/d.cnki.gchau.2024.002027.

[17] Rafi, M. M., Khan, S., & Bhutto, M. A. (2023). Experimental Assessment of Mechanical Properties of Adobe Masonry. Journal of Materials in Civil Engineering, 35(9). https://doi.org/10.1061/JMCEE7.MTENG-15430

[18] Zhou, T., Wang, X., Ma, B., Zhang, Z., & Tan, W. (2022). Seismic performance of new adobe bricks masonry: Design and experiment. Advances in Structural Engineering, 25(2), 277–289. https://doi.org/10.1177/13694332211046349

[19] Bayesteh, H., Safraei, E., & Sharifi, M. (2024). Experimental investigation of the bond strength between GFRP and steel bars and soil-cement. Structures, 65. https://doi.org/10.1016/j.istruc.2024.106761

[20] Cottrell, J. A., Ali, M., Tatari, A., & Brett Martinson, D. (2025). Influence of jute fibre and cement on the mechanical properties of raw earth mortar. Journal of Building Engineering, 108. https://doi.org/10.1016/j.jobe.2025.112935

[21] W. Han, Compressive Performance of Adobe Masonry Strengthened with Glass-fiber Mesh Reinforced Earthen Matrix Composites [D]. (Master's thesis, Dalian Jiaotong University) (2023). DOI:10.26990/d.cnki.gsltc.2023.001298.

[22] F. Cai, Study on mechanical properties of the soil material with chemical reinforcement,(Master's thesis, Dalian Jiaotong University)(2017).https://doi.org/10.26990/d.cnki.gsltc.2019.000297

[23] X. Zhu, M. Su, Y. Wang, T. Ueda, Numerical and theoretical investigation on the constitutive model of graphene-enhanced FRCM composite[J]. Build. Eng. 85 (2024) 108734. https://doi.org/10.1016/j.jobe.2024.108734

[24] X. Liang, Study on the Bonding Performance between Hydraulic Lime Consolidated Earthen Matrix and Raw Earthen Matrix [D]. (Master's thesis, Dalian Jiaotong University)(2024). DOI:10.26990/d.cnki.gsltc.2024.000419.